Advanced probes for edge plasma diagnostics on the CASTOR tokamak

**J Stöckel[1], J Adamek[1], P Balan[3], O Bilyk[1], J Brotankova[1], R Dejarnac[1],
P Devynck[2], I Duran[1], J P Gunn[2], M Hron[1], J Horacek[1], C Ionita[3], M Kocan[4],
E Martines[3], R Panek[1], P Peleman[6], R Schrittwieser[3], G Van Oost[6], F Zacek[1]**

[1] Institute of Plasma Physics, Association EURATOM/IPP.CR, Czech Republic
[2] Association EURATOM-CEA sur la Fusion Contrôlée, France
[3] University of Innsbruck, Association EURATOM/OAW, Austria
[4] Department of Experimental Physics, Comenius University, Bratislava. Slovakia
[5] Consorzio RFX, Associazione EURATOM/ENEA sulla Fusione, Padova, Italy
[6] Department of Applied Physics, Ghent University, Belgium

stockel@ipp.cas.cz
PACS 52.70.Ds

Abstract.
Understanding of underlying physics in the edge plasma of tokamaks requires knowledge of the plasma density, potential, electron and ion temperature, ion flows and their fluctuations with a high spatial and temporal resolution. A family of electric probes, which have been designed and tested for this purpose in the CASTOR tokamak, is reviewed and examples of their performance are given. In particular, we focus on description of the 1D and 2D arrays of Langmuir probes for spatially resolved measurements of the edge turbulence, the Ball pen and emissive probes for direct measurements of the plasma potential, the optimized Gundestrup probe for measurements of parallel and perpendicular ion flow, and the tunnel probe for fast measurement of electron and ion temperatures. Additional information on individual diagnostics is available in the listed references.

1. Introduction

It is widely recognized that the electric probes are important tools for studying edge plasma physics in tokamaks because the required space resolution (in the range of several ion Larmor radii) and a high temporal resolution (of about 1 μs or even better) can be easily achieved. Therefore, they are routinely used on any tokamak facility.

This paper is an overview of probes recently developed to study the edge plasma on the CASTOR tokamak, which is operational in the Institute of Plasma Physics, Prague. The major and minor radii are R = 0.4 m and a = 0.085 m, respectively. The toroidal magnetic field is B_t = 0.6 – 1.2 T, the plasma current I_p = 6 –15 kA and the plasma density n_e < 1.5 10^{19} m^{-3}. The edge plasma on CASTOR is similar to that on larger facilities. The edge density is up to 2 - 3.10^{18} m^{-3}, the electron and ion temperature up to 50 eV. The character of the edge turbulence is also almost identical [1]. The facility itself is quite flexible to operate. Daily, about 50 –70 reproducible discharges can be easily achieved. It can be re-operational just the second day after opening the tokamak vessel to atmospheric pressure, if some modifications are necessary. The duration of the CASTOR discharge is 25 – 35 ms, and this

allows insertion of probes as deep as 20-30 mm inside the Last Closed Flux Surface (LCFS) without any overheating of the probe head and its consequent destruction. This simplifies experiment, because the probes can stay at a fixed position during the whole discharge and complicated reciprocating manipulators need not be exploited as on larger experiments with long pulses.

Because of the above-mentioned reasons, CASTOR is quite suitable for development and testing different kinds of probes, which are surveyed here. The paper is structured as follows: Probe arrays for fluctuation measurements are described in Sec. 2. A novel probe for fast measurement of electron and ion temperatures is described in Sec. 3. Direct measurement of plasma potential, again with a high temporal resolution by using a quite novel approach is described in Sec. 4. Finally, the advanced design of a probe for measurement plasma flows is presented in Sec. 5. Conclusions are given in Sec. 6 and appropriate references are attached as an additional source of information to each diagnostics.

2. Arrays of Langmuir probes

The distribution of plasma parameters in tokamaks along principal directions (radial, poloidal and toroidal) is measured by changing the probe position on a shot-to-shot basis. However, this approach requires sufficiently reproducible discharges and measurements become cumbersome. Moreover, such approach can not be used for investigation of transient processes, such as plasma fluctuations. The above-mentioned complication can be partially overcome by using arrays of Langmuir tips.

Pioneering experiments with the probe arrays were performed by Zweben [2] in the 80s and turbulent structures with a typical lifetime 5-40 µs and a poloidal and radial correlation length of ~ 1 cm have been identified. Systematic measurements of the edge turbulence were carried out in the ASDEX tokamak [3] with an array of 16 tips oriented in the poloidal direction. In spite of a spatially limited picture, the poloidal periodicity of the turbulent events in the scrape-off layer (SOL) (with a typical poloidal wavelength of about 5-15 cm) has been observed. Comparable measurements performed in the CASTOR tokamak [1] with a similar array have demonstrated that the SOL turbulence in small tokamaks is basically of the same nature as in larger machines. Here we focus on recently developed probe arrays labelled further in the text as the rake probe and the poloidal ring.

2.1. Rake probe

The array of Langmuir tips oriented in the radial direction (so called rake probes) is used to determine the radial profiles of edge plasma parameters such as electron temperature, plasma density and floating potential in a single discharge. Two kinds of rake probes used on CASTOR for such purpose are depicted in figure 1. The single rake probe consists of 16 tips spaced radially by 2.5 mm, the length of individual tips is 2 mm. The double rake probe consists of two rows of tips spaced in the poloidal direction by 2.5 mm. The probe head is made of an isolator to avoid short-circuiting of the radial electric field.
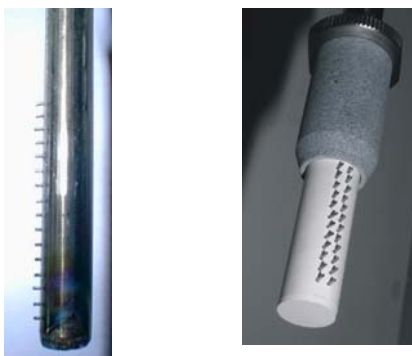

Figure 1. Pictures of the single (left) and the double (right) rake probe.
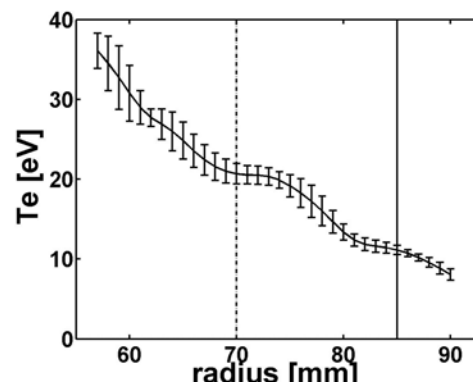
Figure 2. Radial profile of the electron temperature at the edge of CASTOR.

The individual tips can operate in a sweeping mode and the current – voltage characteristic can be measured to determine the radial profile of electron density and temperature (see also [4]. An example of the radial profile of the electron temperature on CASTOR measured by the single rake probe is shown in figure 2. The temporal resolution of this technique is typically 1-2 ms. For fast measurements, e.g. for investigation of plasma turbulence, the tips have to measure either the floating potential, V_{fl} or the ion saturation current, I_{sat}. On CASTOR, a special circuit (see figure 3) is designed to be possible to change mode of operation between shots.
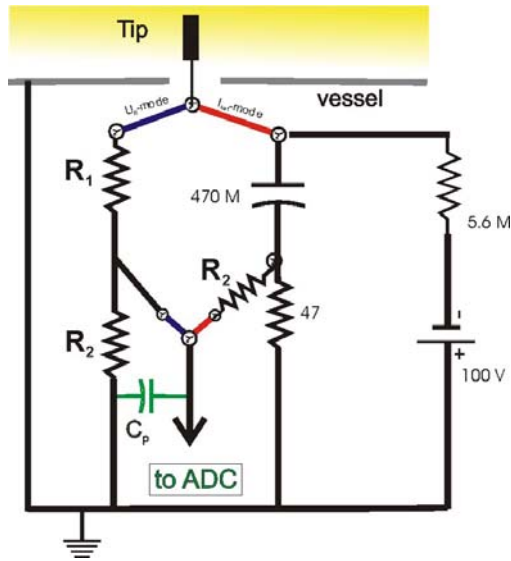
Figure 3. Electric circuit for measurement of the floating potential and the ion saturation current for probe arrays used on CASTOR. The switch is used to change the mode of operation between shots. The voltage divider 1:100 is used to measure the floating potential. The voltage required for measurement of I_{sat} is provided by the condenser 470 µF, which is charged to –100 V between shots via a high internal impedance. The ion saturation current is deduced from a voltage drop on the resistor 47 Ω. The resistor R_2 in the circuit for I_{sat} measurement assures the same frequency bandwidth for both modes of operation.

Typically, R_1 = 660 kΩ, R_2 = 6.7 kΩ, C_p ~300 pF, so the characteristic time constant of the circuits is $\tau = R_2 x C_p \sim 2$ µs, where C_p is the parasitic capacitance. On CASTOR, one power supply serves 16 such circuits.

Examples of measurements in such experimental arrangement are shown in figures 4 and 5, where results of a series of reproducible shots are presented. All the tips of the double rake probe measure either the floating potential V_{fl} or the ion saturation current I_{sat}. The radial position of the rake probe was changed between these shots. The time-average profiles of the floating potential and the ion saturation current are shown in figure 4. As can be seen, the floating potential exhibits a maximum, which is associated with the radial position of the Last Closed Flux Surface located at 70 mm in this particular case. Its gradient $\nabla_r V_{fl}$ has an opposite sign at both the sides of the LCFS and its value is estimated from the slope of dashed lines plotted over the experimental data.
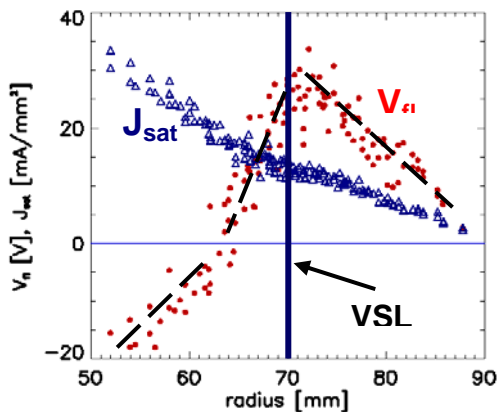
Figure 4. Radial profile of the floating potential (red circles) and the ion saturation current density (blue triangles). Position of the Last Closed Flux Surface (LCFS) corresponds to that of the maximum of V_{fl}, and also to the position of the velocity shear layer (VSL).

Furthermore, the phase velocity of density and potential fluctuation can be derived by a statistical analysis of signals measured by the double rake probe. The result is shown in figure 5. The phase velocity of fluctuations, v_{ph}, is determined from the time shift τ of the cross-correlation function of signals of two poloidally spaced tips of the double rake probe. To determine the time shift τ with a better precision than the sampling rate (1 μs), the cross-correlation function was approximated by a polynomial fit. The phase velocity is calculated by using expression $v_{ph} = d/\tau$, where d is the poloidal separation of the tips.
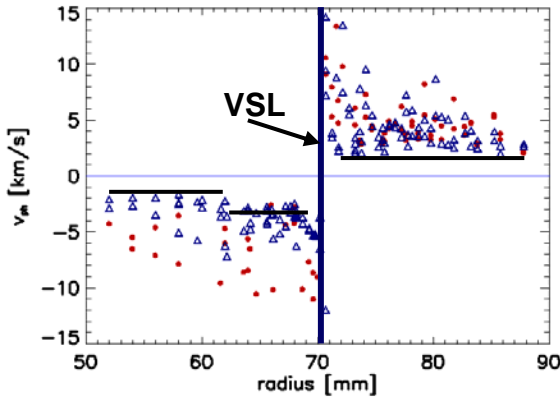

Figure 5. Radial profile of the phase velocity of V_{fl} (red circles) and I_{sat} (blue triangles) fluctuations. The three horizontal lines represent the quantity $-\nabla V_{fl}/B_T$, which is a minimum estimate of the value of the radial electric field at the given range of radii.

As is evident, the phase velocity changes its sign in the proximity of the LCFS and its absolute values are always above the lines $-\nabla_r V_{fl}/B_t$ (shown in figure 5 by three horizontal lines), which represent a minimum estimate of the radial electric field $E_r = -\nabla_r V_{fl}/B_t - \alpha k\nabla T_e/e$ (k is the Boltzmann constant, e is the electron charge and $\alpha \cong 2.5$ for hydrogen plasmas). This implies that the gradient of the electron temperature must be taken into account if a more precise comparison the phase and the $E_r \times B_t$ velocity are required. The time shift of the cross-correlation function is found to be close to zero in the proximity of the velocity shear layer, therefore the phase velocity diverges at this region as is clearly seen in figure 5 and can not be determined by this technique. On the other hand, the position of the VSL is determined with an accuracy of the order ~ 1 mm by this technique. Finally, it is interesting to note that the phase velocity of density fluctuations is systematically lower than that of the potential fluctuations. This observation requires more analysis to be properly explained.

The rake probes are routinely used on CASTOR, namely to monitor the radial profile of the floating potential in ohmic discharges and discharges with edge plasma biasing [5]. In addition, the radial structure of the edge turbulence is measured in this way [6], [7], [8].

2.2 Poloidal ring of electric and magnetic probes
Several probe arrays which allow the investigation of the properties of edge plasma in the poloidal direction were designed and tested on CASTOR. An example of the poloidal ring of 96 Langmuir probes surrounding the whole circumference of the plasma column is shown in figure 6.
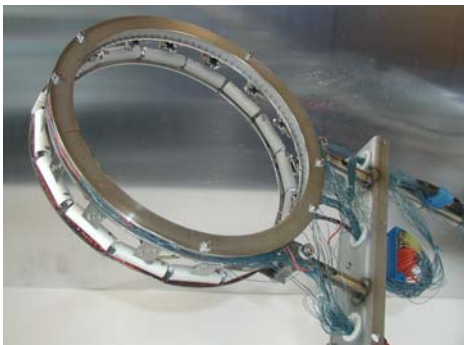

Figure 6. Picture of the full poloidal ring of 96 Langmuir probes. Probes are located at the radius r = 85 mm and their mutual poloidal distance is 5.5 mm. The ring is equipped by 16 Mirnov coils and by 16 Hall sensors to measure the plasma position and to investigate the link between the electrostatic and magnetic fluctuations.

This diagnostic was used to study the poloidal structure of the edge turbulence [6] and its dynamics on CASTOR. Furthermore, the formation of convective cells at edge plasma biasing was identified and described in [9]. More recently, the poloidal ring was used for detail investigation of periodical collapses of the edge transport barrier, which occur in the biasing experiments on CASTOR [8]. Examples of results of the biasing experiments are shown in figure 7 and 8.
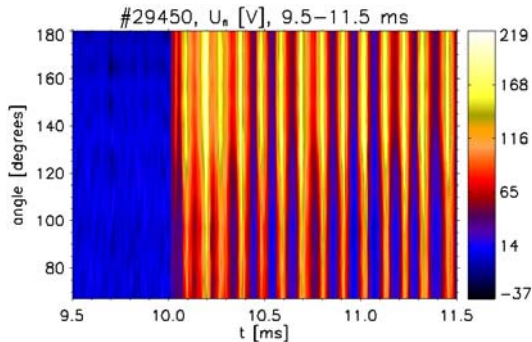
Figure 7. Temporal evolution of the poloidal distribution of V_{fl} at the beginning of the biasing period.
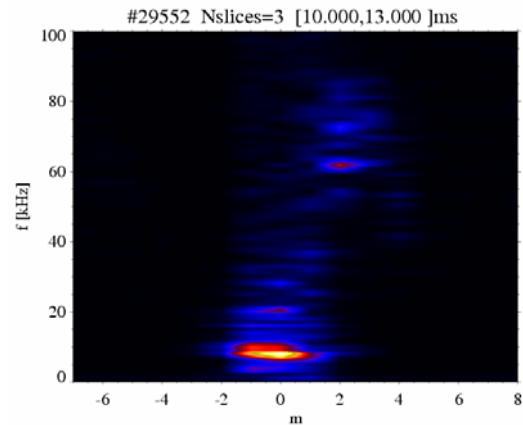
Figure 8. Frequency of magnetic oscillations versus the poloidal mode number m during the biasing period of a discharge.
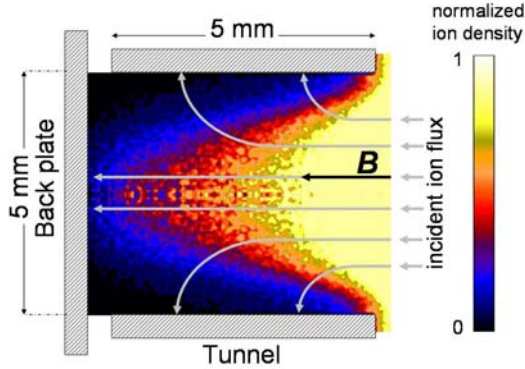
Figure 7 shows the temporal evolution of poloidal distribution of the floating potential measured by the poloidal ring of Langmuir probes along a fraction of the poloidal circumference (in the range of poloidal angles $70^{o} - 180^{o}$). The biasing electrode is located almost at half the plasma radius and biased to +250 V with respect to the tokamak vessel at t = 10 ms. It is clearly seen that the floating potential is strongly modulated with the characteristic period ~ 0.1 ms and it is practically independent of the poloidal angle. Consequently, the poloidal mode number appears to be close to zero. Analysis of magnetic perturbations during biasing reveals a similar feature. Figure 8 shows the frequency spectrum of signals of Mirnov coils versus the poloidal mode number. As can be seen the dominant magnetic mode at biasing is of frequency ~ 10 kHz and the poloidal mode number is close to zero. This observation indicates an electromagnetic character of collapses of the edge barrier at biasing.

In addition, a two-dimensional array of 8x8 tips was used on CASTOR to analyze the properties of the edge turbulence simultaneously in the poloidal and radial direction. An example of the <u>animation</u> of experimental data is attached to this contribution. Coherent structures were identified by a statistical analysis of data in these experiments and results are described in [10].

3. Segmented tunnel probe
A new kind of the Langmuir probe, the "segmented tunnel probe" (STP), was recently developed and tested in CASTOR tokamak in order to provide simultaneous DC measurements of electron and ion temperatures, and parallel ion saturation current density with arbitrarily high temporal resolution. The temporal resolution, 1μs in recent experiments, is limited only by the data acquisition system sampling frequency. This particularity gives the probe a significant potential to be employed in the research of time-dependent phenomena, such as the plasma turbulence, the edge localized modes (ELM's) etc.

Originally, the *tunnel* probe was conceived to measure electron temperature and parallel ion saturation current density at a given spatial location in the tokamak SOL [11], [12], [13]. The probe consists of a hollow-conducting tunnel closed at one end by an electrically isolated conducting back plate, see figure 9. To repel electrons and collect ions, both conductors are negatively biased with respect to the tokamak chamber. The tunnel axis is parallel to the total magnetic field **B**. Ions flowing into the tunnel orifice get un-magnetized by an intense radial electric field in the magnetic pre-sheath and

redistributed between the tunnel and the back plate. The tunnel-to-back-plate ion saturation current ratio is determined by the magnetic pre-sheath thickness in the probe tunnel, $L_{MPS} \propto T_e^{1/2}$, a strong function of T_e. The tunnel probe has been calibrated by means of the two-dimensional "particle-in-cell" code XOOPIC [14]. The code enabled the exploitation of the dependence of the electron temperature on both tunnel-to-back-plate ion current ratio and parallel ion saturation current density, i.e. on the parameters measured directly by the probe.

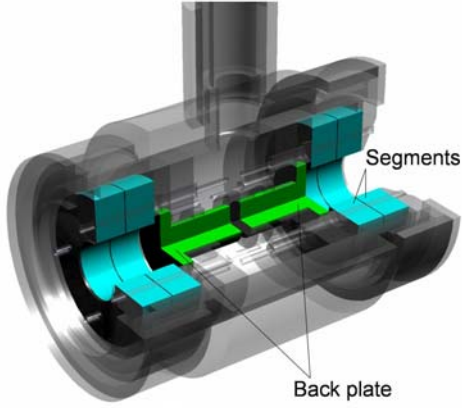**Figure 9.** Schematic drawing of the tunnel probe.
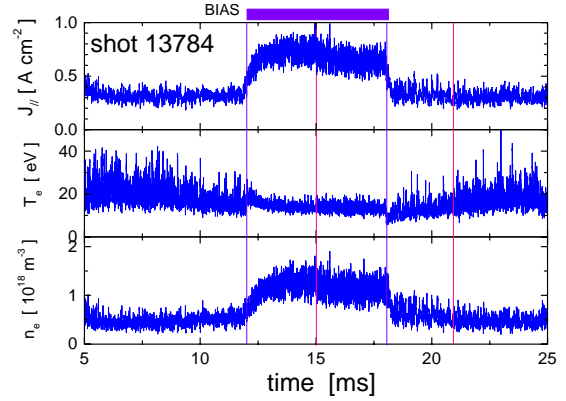
Figure 10. Temporal evolution of parallel current density J_{II}, the electron temperature and density during a shot with plasma biasing.

In figure 10, the temporal evolution of the electron density and temperature (n_e and T_e respectively) and parallel ion saturation current density, $J_{//}$, during a shot with electrode biasing is plotted along a single time axis. These measurements revealed a significant reduction of the electron temperature fluctuations during the biasing phase.

XOOPIC simulations have also shown that the axial distribution of ion flux onto the tunnel decays with a characteristic length scale that is determined by the relative strength of the radial acceleration of ions with respect to the incident parallel ion velocity. The latter is a function of the ion sound speed. Therefore, if we divide the tunnel into two segments, the ion temperature can also be obtained from the ratio of ion current to the first and the second segments, $R_c = I_{seg1}/I_{seg2}$.

To account for the influence of the plasma flows in the SOL, two tunnels are mounted back-to-back in a Mach probe arrangement, figure 11, sampling plasma from both upstream and downstream directions along the total magnetic field. If the plasma flow is not too large, the measured parameters in question are calculated as an average of the upstream and downstream values [15]. Alternatively, floating-Langmuir-probe tips can be installed in front of the tunnel orifice in order to measure turbulent heat and particle fluxes.

Radial profiles of ion and electron temperatures and parallel ion saturation current density for downstream ('d') and upstream ('u') orientation of the STP are shown in figure 12. The profiles of T_e and $J_{//}$ measured by the STP are compared with the ones measured by the rake probe. Due to the pre-sheath effects, the ion temperature in the SOL was found to be considerably higher than T_e (see [16] for more details). The ion and electron temperatures inequality in the SOL and its dependence on the plasma density was studied in detail in a series of discharges with monotonically decreasing density [16]. The ion temperature scales roughly in proportion with $1/n_e$, while the electron temperature remains constant. T_i/T_e varies from ~3 at the lowest density to ~1 at $n_e \cong 10^{18} \, \text{m}^{-3}$. Moreover, periodic modulation of T_i caused by the collapses of the edge transport barrier was recently measured in a series of discharges with a biasing electrode.

Figure 11. Schematic drawing of the probe head of the STP. Two segmented tunnels are mounted back-to-back in a Mach probe arrangement.
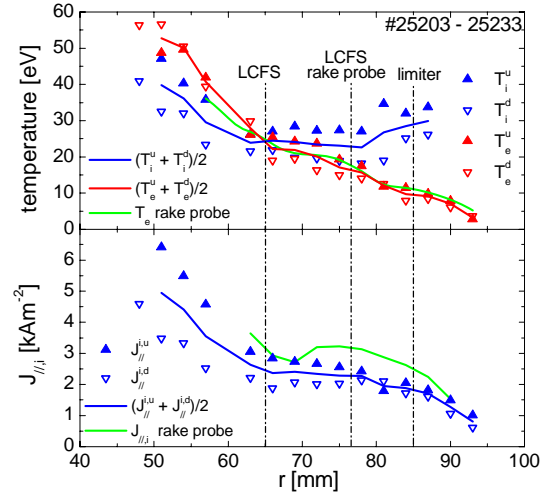
Figure 12. Radial profiles of the electron and ion temperatures (top) and parallel ion saturation current density (bottom) obtained by the STP. T_e and $J_{//}$ are compared with the ones measured by the rake probe.

4. Direct measurement of plasma potential by the emissive and the ball- pen probe

In practice, a simple Langmuir theory is routinely used at the plasma edge for this purpose and the plasma potential Φ is deduced from the floating potential V_{fl} by using the formula

$$V_{fl} = \Phi - \left(\frac{kT_e}{e}\right)\ln(R) \qquad , \qquad (1)$$

where T_e is the electron temperature, k and e denote Boltzmann constant and elementary charge, respectively. The quantity $R = I_{sat}^-/I_{sat}^+$ represents the ratio of the electron to the ion saturation current, respectively. The determination of T_e and R requires measurements of the full *I-V* characteristic, which is, however, not suitable for measurements with time resolution in the range of 1μs, which is usually required to study plasma turbulence in tokamaks.

The basic idea of direct plasma potential measurements by means of electric probes, avoiding the above-mentioned problem, is to adjust R to be equal to one by a proper experimental set-up of the probe. If this is achieved, the floating potential of the probe is equal to the plasma potential, as is evident from Eq. (1).

The standard approach uses the emissive probe, for which the ratio R is expressed as $R = I_{sat}^-$ /(I_{sat}^++I_{ee}), where I_{ee} is the electron emission current. When the emission current balances the electron saturation current ($I_{sat}^- \cong I_{ee}$) the ratio R is adjusted to be close to one. The value of I_{ee} is controlled by probe heating. Successful application of this technique on CASTOR is described in [17]. However, the directly heated emissive probe is too fragile to be routinely used on large-scale facilities, therefore a new concept of indirectly heated emissive probe was developed recently [18]. The probe design (the emitter made of LaB_6 heated by a laser beam) is sufficiently robust to survive typical heat loads at tokamak edge.

The alternative approach, which can be used only in magnetized plasmas, is the concept of the ball-pen probe (BPP) [19]. The probe is designed so that the ratio R can be modified by changing the collecting areas for electrons and ions, taking advantage of the fact that the Larmor radii of electrons and ions are strongly different. The design of the BPP is shown schematically in figure 13. The probe consists of a conically shaped collector made of stainless steel, which is shielded by an insulating tube made of boron nitride. The collector, which is movable inside the tube, is either completely shielded or partially exposed to the plasma. In the ideal case, when the collector is hidden inside the tube, only ions with sufficiently large Larmor radii can reach the collector surface and the collecting area for

electrons is zero. Consequently, the ratio $R = 0$. When the collector is shifted outwards the electron current as well as the ratio R increases. At a certain collector position, the electron and ion currents are expected to be balanced (i.e. $R = 1$). When the collector is fully outside the shielding tube, the probe operates as a conventional single Langmuir probe and measures the floating potential V_{fl}.
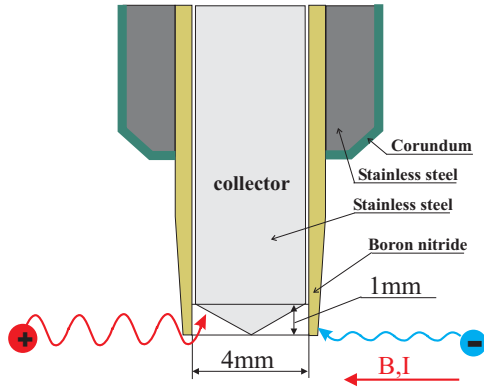
Figure 13. Schematic drawing of the ball-pen probe
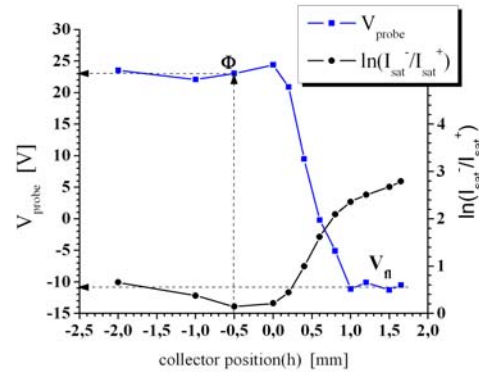
Figure 14. Variation of the collector potential and the logarithm of the R on the collector position

As can be seen from figure 14, we have demonstrated that the ratio R can be significantly modified by moving the collector into the shielding tube. This ratio can be adjusted close to unity ($R \cong 1.1$), if the tip of the conical collector is located slightly inside the shielding tube at the position $h \cong -0.5$ mm.

It should be noted that some experimental observations are not yet fully understood. At first, the collected electron current is always higher than the ion one, even if the collector is completely hidden inside the shielding tube. The presence of electrons at $h < -1$ mm could be explained by an anomalous transport of plasma electrons across the magnetic field lines. Another unexpected feature observed with the collector hidden within the tube is that the probe potential $\Phi^{Ball-pen}$ is practically independent of the collector position for $h < 0$. On the other hand, such findings would be beneficial for the practical use of the BPP in future, because a precise positioning of the collector inside the tube will not be required.

Comparative measurements of the plasma potential with both an emissive and a ball-pen probe in the CASTOR tokamak show a qualitative agreement of both techniques [20]. We conclude that the BPP is a well-suited diagnostic tool for routine measurements of the plasma potential in the edge plasma region of tokamaks, yielding sufficiently high spatial and temporal resolution. Furthermore, the BPP is a very robust construction, surviving even high power loads, so it could also be used in large-scale tokamaks.
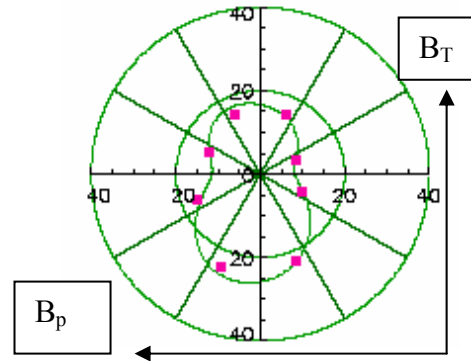
5. Gundestrup probe

Gundestrup probes are used to measure ion flows in magnetized plasmas. The standard design consists of six to twelve conducting pins mounted around an insulating housing in order to obtain a significant variation of the angle between the magnetic field and the probe surface. According to fluid and kinetic modeling, the current density collected by each pin is largely determined by the Bohm-Chodura boundary condition [21]. Despite the rigor of the physics formulation, the precision of flow measurements by Gundestrup probes has so far been limited to large parallel and perpendicular Mach numbers ($|M_{\parallel}|$, $|M_{\perp}| > 0.1$). This is because slight angular misalignments and finite gap width between the pins and the housing cause non-negligible uncertainty of the individual effective collecting areas.

The Gundestrup probe design has been improved ("Ideal Gundestrup Probe", IGP) and tested on CASTOR in order to render it attractive for flow measurements [22]. The ion collecting surface is a nearly continuous cylindrical conductor (made of Cu-tube of diameter 11.7 mm) divided into eight

segments separated by 0.2 mm gaps, as shown in figure 15. The collecting area, determining the radial resolution (2.2 mm) is defined by an insulating quartz sleeve that is slightly shorter than the central conductors. The eight collectors are biased negatively into ion saturation in order to construct polar diagrams with a good temporal resolution.
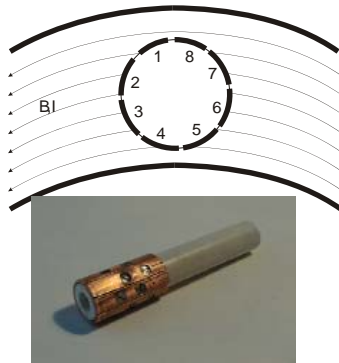
Figure 15. Layout of the Gundestrup probe on the CASTOR. View from the top of the torus

Figure 16. Polar diagram of the ion saturation current measured by individual segments (red squares)

An example of polar diagram of the ion saturation current measure by the Gundestrup probe is shown in figure 16. Asymmetry of the polar diagram in toroidal and poloidal directions indicates existence of parallel and perpendicular flows. The corresponding Mach number can be calculated according fluid model presented in [23].

On CASTOR, an alternative approach for flow velocity measurement was tested. The polar diagram with a high angular resolution was constructed from the signal of a planar probe, rotating with respect to the direction of the toroidal magnetic field lines (rotating Mach probe) [24]. However, the temporal resolution of such probe is limited by the duration of a single revolution, which is typically > 3 ms.

6. Conclusions

Edge plasma diagnostics are inevitably required to understand the underlying physics of processes occurring at the plasma edge of tokamaks, such as the formation of transport barriers, plasma –wall interaction, edge plasma turbulence etc. In particular, radial profiles of plasma density, electron and ion temperature, plasma potential and ion flow velocities have to be measured with a good spatial and temporal resolution. This contribution summarizes results of design and testing such diagnostics on the CASTOR tokamak, which fulfils the majority of requirements mentioned above and allows detailed investigation of the relevant edge physics, in particular the edge plasma turbulence and the role of electric field in plasma confinement. We tried to demonstrate that a relatively small tokamak is suitable for testing novel diagnostics because of its flexibility and routine operation. Additionally, advanced probes' systems described are suitable for measurements in large-scale facilities.

References
[1]   Stockel J, Badalec J, Duran I, Hron M, Horacek J, Jakubka K, Kryska L, Petrzilka J, Zacek F, Heller M V P, Brazilio Z A and Caldas I L 1999 *Plasma Phys Contr Fusion* **41** Suppl. 3A A577.
[2]   Zweben S J et al 1985 *Nucl. Fusion* **25** 543
[3]   Endler M et al, *1995, Nucl. Fusion, 35, 11*
[4]   Van Oost G, Adamek J, Antoni V, Balan P, Boedo J A, Devynck P, Duran I, Eliseev L, Gunn J, Hron M, Ionita C, Jachmich S, Kirnev G, Martines E, Melnikov A, Schrittwieser R, Sylva C, Stockel J, Tendler M, Varandas C, Van Schoor M, Vershkov V and Weynants R 2003 *Plasma Phys. Contr. Fusion* **45** 621-643
[5]   Popov Tsv K, Stockel J, Dejarnac R, Dimitrova M, Ivanova P and Nadyenova Tsv 2006 *Journal of Physics Conference Series*, this Proceedings
[6]   Devynck P, Bonhomme G, Martines E, Stockel J, Van Oost G, Voitsekhovitch I, Adámek J, Azeroual A, Doveil F, Duran I, Gravier E, Gunn J and Hron M 2005 *Plasma Phys. Contr. Fusion* **47** 269-280
[7]   Bencze A, Berta M, Zoletnik S, Stockel J, Adamek J and Hron M 2006 *Plasma Phys. Contr. Fusion* **48** S137-S153
[8]   Spolaore M, Martines E, Brotanková J, Stockel J, Adamek J, Dufková E, Duran I, Hron M, Wenzettl V, Peleman P, Van Oost G, Devynck P, Figuerredo H and Kirnev G 2005 *Czech.J.Phys.* **55** 1597-1606
[9]   Stockel J, Devynck P, Gunn J, Martines E, Bonhomme G, Voitsekhovitch I, Van Oost G, Hron M, Duran I, Stejskal P, Adamek J, Weinzettl V and Zacek F 2005 *Plasma Phys. Contr. Fusion* **47** 635
[10]   Martines E, Hron M and Stockel J 2002 *Plasma Phys. Control. Fusion* **44** *351*
[11]   J.P. Gunn et al 2001 *Phys. Plasmas* **8** 1995
[12]   Gunn JP, Devynck P, Pascal JY, Adamek J, Duran I, Hron M, Stockel J, Zacek F, Barina O, Hrach R, Vicher M and Van Oost G 2002 *Czech. J. Phys.* **52** 1107-1114
[13]   Gunn JP, Panek R, Stockel J, Van Oost G and Van Rompuy T, 2005 *Czech.J.Phys.* **55** 255-263
[14]   J. Verboncoeur et al. 1995 *Comput. Phys. Commun.* **87**, 199
[15]   Kocan M, Panek R, Gunn J P, Stockel J and Skalny J D 2005, *In Proc of 32nd EPS Conference on Plasma Phys. Tarragona, ECA,* Vol.**29C**, P-2.082
[16]   Kocan M, Panek R, Stockel J, Hron M, Gunn J P and Dejarnac R, 2006 Int. Conf. Plasma Surface Interaction, Hefei, China P3-59, To be published in J. Nucl. Mater.
[17]   Schrittwieser R, Adamek J, Balan P, Hron M, Ionita C, Jakubka K, Kryska L, Martines E, Stockel J, Tichy M, and Van Oost G 2002 *Plasma Phys. Contr. Fusion* **44** 567-578
[18]   Schrittwieser R, Sarma A, Amarandei G, Ionita C, Klinger T, Grulke O, Vogelsang A, and Windisch T 2006 *Physica Scripta* **T123** 94-98
[19]   Adamek J, Stockel J, Hron M, Ryszavy J, Tichy M, Schrittwieser R, Ionita C, Balan P, Martines E and Van Oost G 2004 *Czech.J.Phys.* **54** Supl. C C95
[20]   Adámek J, Stöckel J, Ďuran I, Hron M, Pánek R, Tichý M, Schrittwieser R, Ionita C, Balan P, Martines E and Van Oost G, 2005 Czech.J.Phys. **55** 235-242
[21]   Gunn JP, Boucher C, Devynck P, Duran I, Dyabilin K, Horacek J, Hron M, Stockel J, Van Oost G, Van Goubergen H and Zacek F, 2001 *Physics of Plasmas* **8(5)** 1995-2001
[22]   Gunn J, Stockel J, Adamek J, Duran I, Horacek J, Hron M, Jakubka K, Kryska L, Zacek F and Van Oost G 2001 *Czech. J. Phys.* **51** 1001
[23]   Van Goubergen H et al 1999 *Plasma Phys. Contr. Fusion* **41** L17
[24]   Dyabilin K, Hron M, Stockel J and Zacek F 2002 *Contrib. Plasma Physics* 99-108